

## **DEVELOPMENT OF A YARN GUIDING AND IMPREGNATION TECHNOLOGY FOR ROBOT-ASISSTED FIBER MANUFACTURING OF 3D TEXTILE REINFORCEMENT STRUCTURES**

Danny Friese, Institute of Textile Machinery and High Performance Material Technology (ITM) –  
Technische Universität Dresden, Germany, danny.friese@tu-dresden.de

Johannes Mersch, ITM – Technische Universität Dresden, Germany, johannes.mersch@tu-dresden.de

Lars Hahn, ITM – Technische Universität Dresden, Germany, lars.hahn@tu-dresden.de

Chokri Cherif, ITM – Technische Universität Dresden, Germany, chokri.cherif@tu-dresden.de

### **ABSTRACT**

An innovative technological approach will promote a greenhouse-gas-reduced construction method that utilizes the full potential of high-performance textile-reinforced concrete by means of novel and improved construction strategies. To this end, natural load transfer principles, e.g., from botany, are used to achieve maximum material efficiency. The developed highly flexible robotic manufacturing technology is used to realize spatially branched 3D textile reinforcement structures. The paper presents the fiber-gentle and leakage-free yarn guiding and impregnation technology, which is essential for the realization of freely formed 3D textile reinforcements using the robotic 3D yarn deposition technology.

### **KEYWORDS**

3D textile reinforcement structures; yarn impregnation tool; robot-assisted yarn deposition technology; biological inspirations; textile reinforced concrete, CRC/TRR280

### **INTRODUCTION**

Sustainability has become a critical consideration in the field of civil engineering, particularly in the construction industry, where buildings and infrastructure are responsible for a significant amount of resource consumption, energy use, and carbon emissions (Beyond Zero Emissions, 2017). Almost 37% of global carbon dioxide (CO<sub>2</sub>) emissions are attributable to the lifetime use of buildings (UN Environment Programme, 2021). The production of ordinary cement as the main component of concrete in the construction industry causes the emission of greenhouse gases such as CO<sub>2</sub>. Approximately 9% of global CO<sub>2</sub> emissions are produced by the construction sector during the construction phase of concrete-based buildings (Crippa et al., 2019). To address these issues, innovative solutions such as textile-reinforced concrete (TRC) and in particular carbon concrete composite (CCC) have been developed to reduce the negative impacts of steel-reinforced concrete (SRC) as the world's most important building material and the second most used resource in the world, surpassed only by water (Gagg, 2014). Using non-corrosive TRC drastically reduces the need for concrete (Scheerer, 2015). The idea behind TRC is based on the established principles of reinforced concrete, where the concrete matrix is highly resistant to pressure and is easy to cast into many different forms using locally available materials (Scheerer, 2015). Concrete's relatively low tensile strength is compensated by the use of higher tensile strength reinforcements like steel or technical fabrics. Steel-reinforced concrete has been researched and used for almost two centuries and is one of the cornerstones of the modern construction industry. The corrosion resistance of common reinforcement textiles, such as carbon fiber, is better than that of steel reinforcement. This has a positive effect on their long-term strength and the required thickness of the concrete cover (Cherif, 2016). In addition, carbon fiber (CF) is characterized by long-term resistance in alkaline environments, a low density of 1.77 g/cm<sup>3</sup> (whereas that of construction steel

is 7.8 g/cm<sup>3</sup>), high geometric flexibility, and high mechanical strength. Regarding the latter, the tensile strength of CF, depending on fiber type, is up to 4,000 N/mm<sup>2</sup>, compared to a yield strength of about 500 N/mm<sup>2</sup> for structural steel (Deutsches Institut für Normung e.V., 2009 - 08; Friese, Scheurer, et al., 2022; Kulas, 2013). As TRC combines low weight and high strength with corrosion resistance, currently the two main applications of TRC are the retrofitting of existing building structures (Koutas et al., 2019; Schladitz et al., 2009) and the production of precast elements (May et al., 2019). Facades and elements for simple buildings such as pavilions or garages are more specific examples of TRC precast elements (Raupach & Morales Cruz, 2016; Scholzen et al., 2015). TRC has even been used to construct several pedestrian and cyclist bridges, some with prefabrication and some with on-site casting (Adam et al., 2020; Helbig et al., 2016). Furthermore, the CUBE in Dresden (Germany) is the first house worldwide to be built entirely using TRC (Tietze et al., 2022). Currently established textile reinforcements are similar in form, function, and application methods to steel reinforcements (Curbach, 2019). Novel design strategies for the material-minimized use of TRC are under development and aim to realize biologically inspired load transfer principles from nature (e.g., botany) to further scale down concrete consumption (Beckmann et al., 2021). The transition zones of peltate-shaped leaves, i.e., leaves where the petiole is attached on the abaxial side of the lamina, show promising strengthening structures for biomimetic load-bearing components (Wunnenberg et al., 2021). Although warp-knitting technology is currently the standard for the highly productive production of textile reinforcement structures such as grid-like textile reinforcement mats, textile machine technology reaches its geometric manufacturing limits when it comes to biologically inspired three-dimensional (3D) textile structures (Hahn et al., 2023). The production of botanically inspired and thus complex and inner-branched textile reinforcing topologies, which are urgently required, is only realizable by the unsurpassed flexibility of the robot-assisted direct yarn deposition technology (Friese, Hahn, & Cherif, 2022). Therefore, the industrial robot makes use of its six motion axes and various additional functional modules in order to guide and deposit the pre-impregnated or even freshly impregnated roving, i.e., a continuous multifilament yarn. Main modules are the yarn deposition tool for yarn guiding and impregnation and the work piece carrier for yarn fixation until full structure consolidation (Friese, Scheurer, et al., 2022). The literature shows a multitude of impregnation processes regarding the robotic yarn deposition – some with in-line impregnation and some with out-of-line impregnation – but none of them is characterized by a flexible, closed, and semi-hermetic in-line impregnation module with impregnation properties suitable for the manufacturing of biologically inspired, highly branched 3D textile reinforcement structures (Knippers et al., 2016; Mechtcherine et al., 2020; Minsch et al., 2018).

In this context, this paper aims to explore the impregnation potential of carbon fiber heavy tows (CFHT) for the robot-assisted processibility by means of an individually customized impregnation box. The focus is on the load capacity of the fibers and the mobility of the impregnation module itself through a slim and enclosed design.

## **EXPERIMENTAL INVESTIGATION**

This paper provides an overview of the influence of various functional elements within the impregnation box (I-Box) on the optimum impregnation of yarns with thermosetting resins. The influence of specific impregnation parameters (see Table 3 in Methods) on the impregnation quality of roving cross sections and thus tensile strength was determined by tensile testing, microscopic analyses, and gravimetric as well as ashing investigations. In addition, this work provides a first insight into the excitation of the impregnating agent by ultrasonic vibration and its effect on the impregnation behavior and tensile strength of impregnated CFHT. Another focus of the study is the technological development process of a customized I-Box according to the requirements of the robot-assisted yarn deposition technology.

### **Materials**

The fiber material used in this study is listed in Table 1 and produced by Teijin Carbon Europe GmbH (Wuppertal, Germany). The CFHT has a yarn count of 3,200 tex with single filaments each 5–10 microns in diameter. The CF is a man-made fiber primarily produced from the synthetic polymer

polyacrylonitrile (PAN). Due to the high anisotropic molecular structure this technical fiber has favorable properties for the reinforcement applications and thus for the strengthening of concrete structures (Cherif, 2016). CF offers the highest resistance to alkaline environments, for example when embedded in concrete, and the highest Young’s modulus as well as tensile strength in fiber axial direction compared to other technical fibers in the scope of concrete reinforcement, such as alkali-resistant glass fiber, basalt fiber, or aramid fiber (Cherif, 2016; Wulfhorst et al., 2014).

Table 1: Properties of the Carbon Fiber Heavy Tows (Teijin Limited, 2020)

	Density in g/cm <sup>3</sup>	Sizing agent	Modulus of elasticity in GPa	Tensile strength in MPa	Ultimate strain in %
Tenax®-E STS40 E23	1.77	Based on epoxy resin	250	4,300	1.7

The physical properties of the impregnation agent produced by SIKA Deutschland GmbH (Stuttgart, Germany) are shown in Table 2. The impregnation agent applied in this investigations shows a structurally viscous behavior in the still uncrosslinked, liquid state of the resin-hardener system; see investigations of (Meier, 2017). Main functions of the impregnation agent are the increase of the outer and inner bond strength of the roving and the improvement of durability of reinforcing fiber materials as well as of the resistance to external influences. The impregnation material also improves handling properties during processing and protects the textile reinforcement from external influences during transport or processing by ensuring that the structural geometry of the fiber orientation can be maintained (Hahn, 2020). Finally, reinforcing fibers can withstand higher tensile forces, increasing their strength (Kulas, 2013).

Table 2: Impregnation agent (Sika Deutschland GmbH, 2016)

	Density in g/cm <sup>3</sup>	Modulus of elasticity in GPa	Tensile strength in MPa	Ultimate strain in %
Biresin CR84/CH94-2	1.14	3.2	85	4.2

## Methods

The current robot-assisted production technology for yarn direct deposition under development is shown in Figure 1. The current technology is suitable for two-dimensional reinforcement structures, e.g., grid-like reinforcement mats. Figure 1b shows the current yarn guiding and impregnation module used for the yarn impregnation and direct yarn deposition. The technology under development will be able to manufacture simple planar reinforcement structures as well as more complex three-dimensional reinforcement structures with inner branchings and a hierarchical construction, such as needed for column-like concrete components and reinforcement cages. To be able to implement this target application the robot-assisted technology requires a fundamentally new module structure with a focus on maximum mobility and the possibility to deposit the impregnated yarn in space, as can be achieved with a 3D yarn fixation module by (Friese, Hahn, & Cherif, 2022); see Figure 1c. The new impregnation module (Figure 1d) is based on the identified technological requirements (see Table 5 in chapter “Technological and constructive development of impregnation module”) and the on-site requirements such as reinforcement design and position accuracy of the reinforcement structure that must be taken into account.

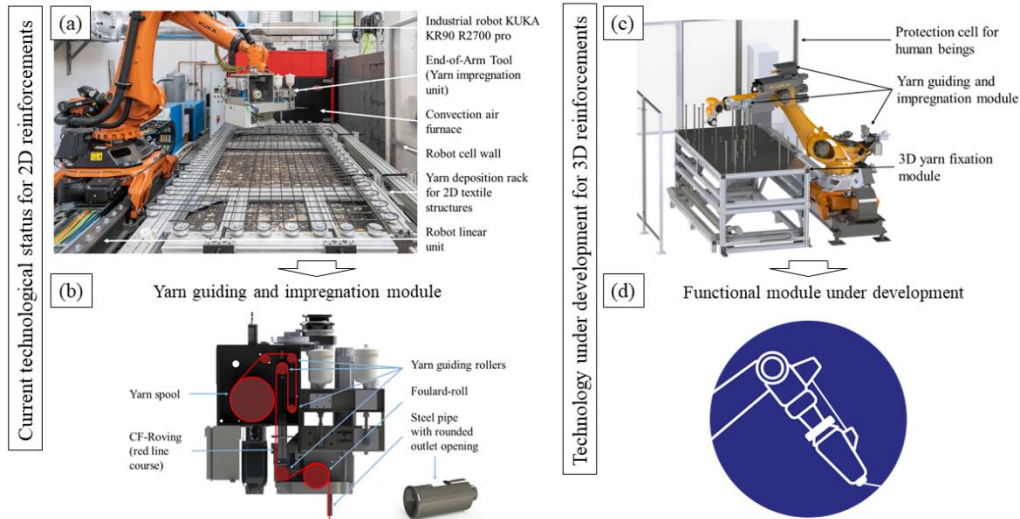


Figure 1: Current robotic production technology for direct deposition of yarn (a) and robotic production technology under development (c) with the yarn guiding and impregnation module (b) as well as the requirements for the I-Box under development (d)

To ensure complete, homogeneous, and damage-free yarn impregnation, a comprehensive experimental examination program was conducted to fit the best impregnation design, which is influenced by specific structural and process parameters. Different variable parameters have been investigated particularly with regards to their impact on the impregnation quality and the mechanical properties – especially the tensile strength. Table 3 lists the parameters for closer examination. The choice of parameters depended on several factors that are essential for the integration of the I-Box into the robot-supported direct yarn deposition process:

- a) Closed and semi-hermitic topology
- b) Functional element to improve impregnation
- c) Minimal filament damage
- d) Probability of plant integration
- e) Minimum required installation space

Table 3: Variable parameters for impregnation analysis

	Variables						
Term	I: Yarn feed direction	II: Yarn tensile force	III: Number of guide pulleys	IV: Diameter of guide pulley	V: Position of guide pulley	VI: Orientation of yarn guidance	VII: Stimulation via supersonic
Principal illustration		(a) 500 cN (b) 750 cN (c) 1000 cN		(a) 10 mm (b) 20 mm (c) 30 mm	S1 S2 S3 S4 S5 	(a) (b)	(a) (b)

The supply direction (I) of the yarn was either vertical or horizontal. The yarn tensile force (II) was either 500, 750, or 1,000 cN. Impregnation modifications (III) were realized without and with up to three guide pulleys, where the smallest diameter of a guide pulley (IV) was 10 mm, the middle diameter 20 mm, and the biggest diameter 30 mm. The position of the pulley (V) was evenly distributed over the length of 180 mm – following every 30 mm was a positioning point for a pulley. The yarn was guided (VI) above or below the pulleys or by a combination of both. Since the rotational axes of the spreader rollers were not on the same level as the yarn infeed and outfeed, this feature also had an indirect influence on the impregnation quality (see Figure 2). Finally, the effect of an external vibration source (VII) was studied by the direct comparison of an undeflected, straight running yarn with and without supersonic impact. Parameters such as the geometry of the I-Box, the impregnation velocity, or the used material were constant during the entire examination process.

The experimental design provided for at least seven test specimens per test configuration, so that the statistical significance was given. After initial tactile tests, it was shown for the configurations in which functional elements are used that the parameters *number of rolls*, *roll size*, *yarn orientation*, and *yarn*

*feed* direction have only an indirect influence on tensile strength. These influencing factors, subsequently referred to as sub-parameters, change the functional arc length, which in turn has a direct influence on the impregnation properties and thus on the tensile strength. The functional arc length describes the length over which the yarn has direct contact with the functional element, i.e. the spreader roller. As a result of the preliminary investigation, it could be determined that the more the roving is spread by one or more functional elements and the flow path is shortened accordingly or the roving impregnation is improved by an alternative physical process, the higher the resulting tensile strength is assumed to be. The tensile strength is chosen as a parameter for the evaluation of the mechanical performance in the subsequent evaluation of the test results. The aim of the experimental impregnation tests is to achieve a maximum tensile strength of the impregnated, consolidated CF roving, which comes as close as possible to the single filament strength with its maximum tensile strength of 4.300 N/mm<sup>2</sup> (see Table 1). As a result, the statistical experimental design shown in Table 4 is obtained with ten research series, each with varying parameter configurations. The objective is to identify the most optimal I-Box modification to achieve the maximum tensile strength of the impregnated CF roving. The geometric dimensions of the I-Box used for the experimental investigations are shown in Figure 2.

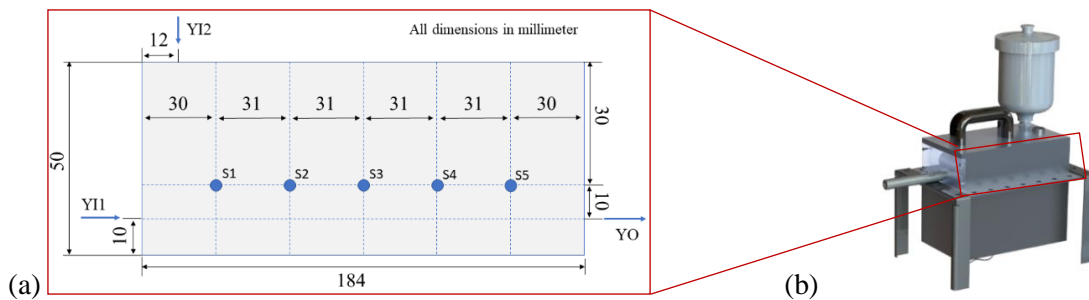
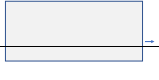



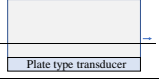





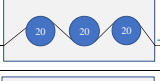








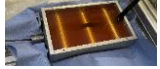


Figure 2: (a) Longitudinal section of the I-Box with the internal geometric dimensions: S – Rotation axis of spreading pulley, YI – Yarn infeed, YO – Yarn outfeed; (b) I-Box used for experimental tests

The laboratory I-Box is equipped with four different M12 x 1.75 metric ISO threads – two threads for the yarn infeed (horizontal and vertical), one thread for the yarn outfeed, and one thread for the flow cup with the impregnation agent. The two different yarn infeed directions were chosen to allow design freedom in terms of optimum alignment on the robot flange during the subsequent design development process of the impregnation module. The inner dimensions of the I-Box are executed almost uniformly to enable a systematic evaluation. Furthermore, following expert advice, the bottom of the I-Box was made to a very small thickness of 2 mm to allow the transmission of the vibrations of the ultrasonic generator (Dreyer, 2022). The impregnation path length (184 mm) as well as the tube-like roving infeed and outfeed with a hole diameter of 2.5 mm remained unmodified throughout the whole experimental testing. All batches in the study and their configuration are shown in Table 4. For all batches, the impregnation tests were carried out with a yarn tensile force of 5.0 N. Preliminary investigations have shown that this force level is suitable in terms of low yarn damage due to roving guide process and of yarn tension, and therefore low yarn slag.

In addition, in the case of V5, yarn tension of 7.5 N and 10.0 N were also investigated in order to determine the dependence of the tensile strength on the yarn tension. The yarn tensile forces correspond to steady-state yarn tensions of 2.7 N/mm<sup>2</sup> for 5.0 N, 4.05 N/mm<sup>2</sup> for 7.5 N, and 5.4 N/mm<sup>2</sup> for 10.0 N based on a yarn count of 3,200 tex.

Table 4: Design of experiments according to the previously identified parameters

Batch	Impregnation variation		Batch	Impregnation variation	
	I-Box configuration	I-Box in process		I-Box configuration	I-Box in process
V1			V6		
V2			V7		
V3			V8		
V4			V9		
V5			V10		

The continuously uniform roving tensile force is applied by an electronically controlled unwinder, which also stores the spool with the CF roving (see Table 3). A torque-controlled unwind and rewind unit is used to precisely activate the predefined yarn force which reflects the production process. After the roving passed the I-box, the freshly impregnated roving is placed on a reel. The reel offers four placement sections with an identical length of 508 mm for the roving placement. Thus, after the complete consolidation, the impregnated roving is in a straight position so that the test specimen can be removed for testing. The rovings can be placed next to each other, enabling the placement of several test series next to each other. A servomotor drives the reel with a constant rotation speed of approximately 3 rpm, which corresponds to a translative velocity of 0.1 m/s. This production speed is constant over all tests to ensure comparability between the individual test series. The rotational speed of the servomotor is controlled via a frequency generator and can be regulated continuously. Figure 3 shows the experimental setup for the production of specimens under varying production parameters.

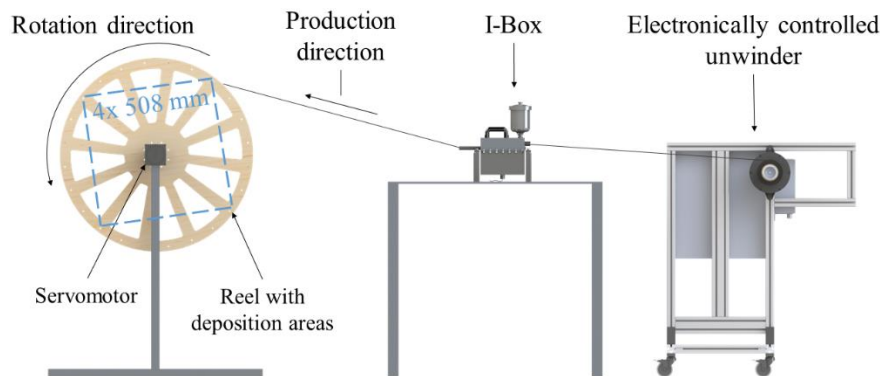


Figure 3: Experimental setup for specimen production with varying functional elements.

The analysis of the experimental testing takes place through specific testing methods for composites. The resulting tensile strengths and the fiber volume fractions of the individual test batches are of essential importance for the further usability in the technological development of the impregnation unit for the robot-supported yarn deposition technology. For only structures with a high tensile strength and stiffness resulting from the parallel fiber arrangement and the high fiber volume content that can thus be achieved can enable highly stressed composite components (Cherif, 2016).

The characterization of the load-bearing capacity of the impregnated CF rovings follows in accordance with the standardized testing method of DIN EN ISO 10618 (DIN Deutsches Institut für Normung e.V., 2004). The tensile strengths of the consolidated CF rovings enable conclusions to be drawn regarding the impregnation process and the resulting quality for each impregnation configuration. The clamping

zones of the specimens need to be prepared before testing in order to homogeneously transfer the testing force from the clamps to the specimen and to avoid the risk of jaw breaks. Therefore the ends of the specimens are resinated on a length of 125 mm in an additional manufacturing step. The free length of the tested roving is 200 mm. Before testing the specimens are heat-treated for 2 hours at 90°C for a fully consolidated matrix. According to DIN EN ISO 291 the specimen needs to be stored in a standard climate for at least 24 h before testing (DIN Deutsches Institut für Normung e.V., 2008). The test setup for the tensile strength testing is shown in Figure 4. All tensile tests were performed with the Zwick Z100 uniaxial tensile testing machine. The entered force and elongation were recorded during the test at a test speed of 3 mm per minute. The applied pre-force of 10 N ensures the compensation of any appearing forces or negative impacts during specimen insertion. During testing an optical elongation measuring system detects the length change of the specimen. The testing parameters are shown in Figure 4c.

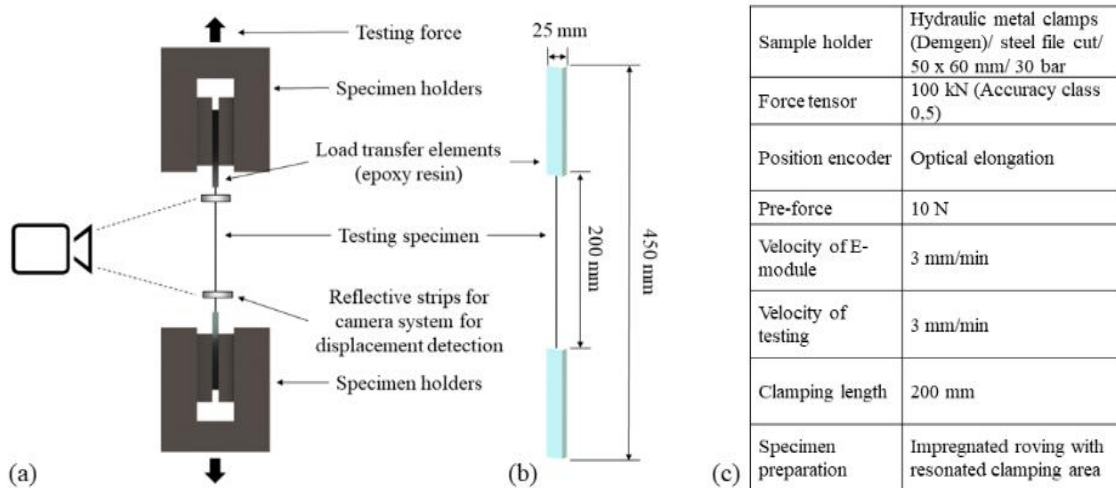


Figure 4: (a) Test setup for uniaxial tensile strength testing; (b) according to specimen geometry; (c) pre-adjustments for the tensile strength testing method according to DIN EN ISO 10618

The characterization of the fiber volume fraction (FVF) of the impregnated CF roving follows the standardized testing method DIN EN ISO 1172 (DIN Deutsches Institut für Normung e.V., 2022). Substantial information about the impregnation quality and thus of the intensity are derivable by means of the determination of the fiber volume fraction. Hence, statements can be made regarding the impregnation configuration with the highest performance in connection with the tensile strength. For the determination of the FVF, the test specimens are cut into pieces with a length of nearly 30 mm. A fireproof crucible made of ceramic is filled with the cut specimens with a mass of 2 to 20 grams per crucible. Then the crucible is weighed to determine the initial mass ( $m_1$ ) of the research substance. Afterwards the crucible with the specimens is dried at 100°C for 60 minutes and the dried specimens are weighed to obtain the dry mass ( $m_2$ ). Then the crucible is placed in the muffle furnace at 625°C until there is no more change in mass. Then the crucible with the calcination residue is weighed again to get the final mass ( $m_3$ ). The schematic process of this ashing test is shown in Figure 5.

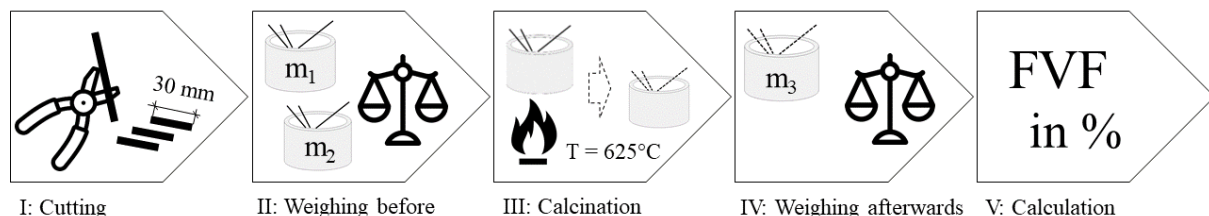


Figure 5: Schematic for determination of the fiber volume fraction (FVF) by means of ashing test

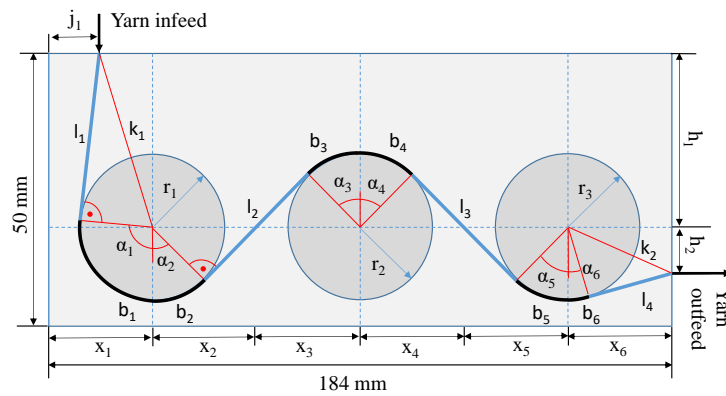
Three individual measurements are taken for each test specimen, resulting in an average value. The following calculation path was used to determine the FVF:

$$M_{CF} = \frac{m_3 - m_1}{m_2 - m_1} * 100 \quad (\text{Eq. 1}) \quad \vartheta = \frac{\rho_M}{\rho_{CF}} \quad (\text{Eq. 2}) \quad \varphi_{CF} = M_{CF} \cdot \vartheta \quad (\text{Eq. 3})$$

Where:

- |         |  |                  |   |
|---------|--|------------------|---|
| $m_1$ : | Initial mass of the crucible (in g)                              | $M_{CF}$ :       | Mass fraction carbon fiber (wt. %)                    |
| $m_2$ : | Initial mass of the crucible with the dried test specimen (in g) | $\vartheta$ :    | Conversion factor (-)                                 |
| $m_3$ : | Final mass of crucible with the calcination residue (in g)       | $\rho_M$ :       | Density of impregnation agent (in g/cm <sup>3</sup> ) |
|         |  | $\rho_{CF}$ :    | Density of carbon fiber (in g/cm <sup>3</sup> )       |
|         |  | $\varphi_{CF}$ : | Fiber volume fraction (in vol. %)                     |

In preparation for the evaluation of the test results, the resulting functional arc length was determined as an influencing variable for each test variant. In the subsequent analysis, this variable will be used to determine the extent to which the position(s) of the roller(s), their diameter or their number have a significant effect on the tensile strength. An example calculation of the functional arc length for variant 10 is shown in Figure 6.



Parameter	$r_1$	$r_2$	$r_3$	$h_1$	$h_2$	$j_1$	$x_1$	$x_2$	$x_3$	$x_4$	$x_5$	$x_6$	Functional arc length $b_1 = b_1 + b_2 + b_3 + b_4 + b_5 + b_6$
Value [in mm]	15	15	15	30	10	12	30	31	31	31	31	30	54.8

Figure 6: Trigonometrical determination of the functional arc length using batch V10 as an example

### Technological and constructive development of impregnation module

At the beginning of the development process was a comprehensive analysis stage in order to gather all essential requirements for the impregnation module under development. In the course of this initial development phase a profile of requirement features was created with associated requirement types and quantitative values or explanatory notes. Three different requirement types prioritize the various demands towards the construction, as certain required features may be mutually exclusive and therefore not all requirements can be met. The requirements for the yarn impregnation module are shown in Table 5.



Table 5: Requirements for functional module “Impregnation Box” (I-Box)  
(Requirement type: F – Fixed / M – Minimum / D – Desired)

Features	Type	Values, data explanations
Geometry	F	Minimum assembly space; closed geometry of the I-Box
Universality	F	Flexibility in material selection (impregnation agent, fiber material, yarn count)
Modularity	F	Modular design for quick changeability of I-Box
Reusability	F	Simplicity in cleaning
Yarn impregnation process	M	Homogeneous, damage-free roving impregnation; validation via tensile tests, ashing tests, grinding patterns
Impregnation return	D	Impregnation circuit (improvement of mixing and avoidance of suspended matter deposition)
Delivery tube	M	Length: 50–150 mm; maximum outer tube diameter: 20 mm; minimum hole diameter: 2.2 mm (depending on yarn), high bending stiffness: displacement of the yarn outfeed center under load less than 1 mm
Process temperature	F	$T_{\text{Process}} < 160^{\circ}\text{C}$ according to the technical data sheet of Biresin CR84/CH120-6 (Sika Deutschland GmbH, 2016)

The development of the I-Box must take into account the requirements from the analysis phase, the needs of the construction industry, and the biologically inspired structures to be created. Requirements such as the semi-hermetic nature of the I-Box, which favors high freedom of movement without leakage, and the minimal installation space of the tool attached to the robot flange, have a high priority. In Figure 7 the resulting functional structure for the I-Box is depicted. The main function is the yarn impregnation. Sub-functions are the regulation of signals and penetration of the roving with impregnation agent.

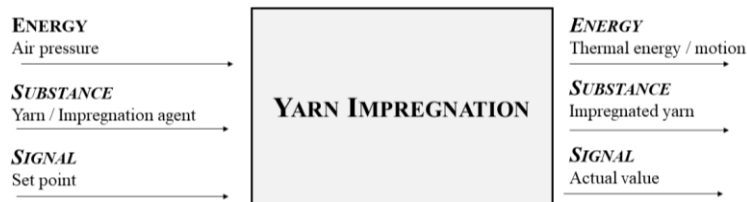


Figure 7: Functional structure of the yarn impregnation module

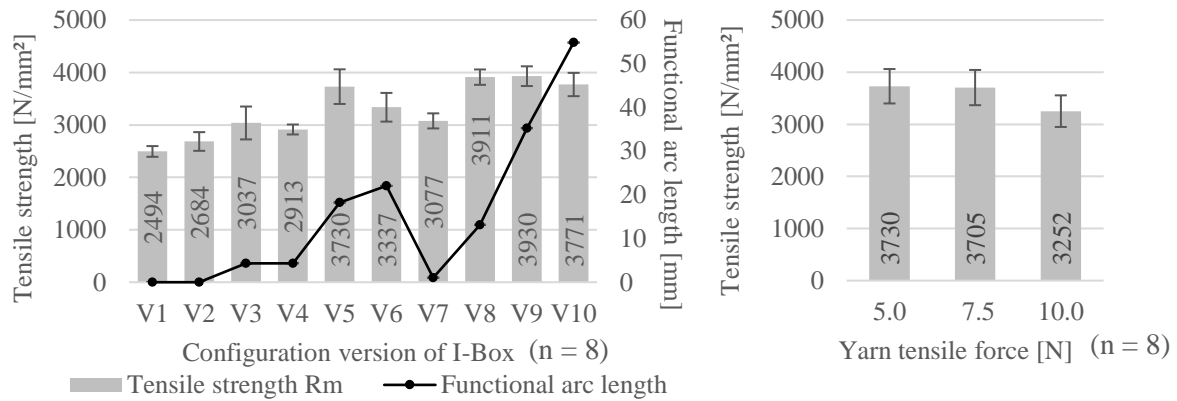
Among the already mentioned constructive requirements, technological specifications regarding the yarn impregnation process under limited conditions (i.e., closed cavity and the restricted installation space) must also be incorporated into the development process.

The results of the experimental research of impregnation configuration in favor of highest tensile strength properties of the carbon roving are given in the following section. The derived constructive solutions for the new impregnation box are subsequently described. Based on the identified catalogue of requirements as well as the functional structure, comprehensive solution approaches for the individual sub-functions as well as the overall function were collected in a morphological box, so that solution variants were then set up. The solution variants were then evaluated on the basis of weighted criteria so that a preferred solution was finally obtained.

## RESULTS AND DISCUSSION

As with the previous technological investigations, the results and the corresponding conclusions refer to the consideration of an impregnation box as an elementary component of the robot-assisted direct yarn delivery technology. In general, the evaluation of the experimental results concludes that there are two main factors influencing the roving tensile strength – the *yarn tensile force* occurring in the process and the *functional arc length*. Figure 8 shows the dependency of the tensile strength on the functional arc length and the yarn tensile force (sample size  $n = 8$ ). As can be seen in Figure 8a, the highest tensile strength of 3,930 N/mm<sup>2</sup> (V9) can be reached when the functional arc length is high (35 mm). The

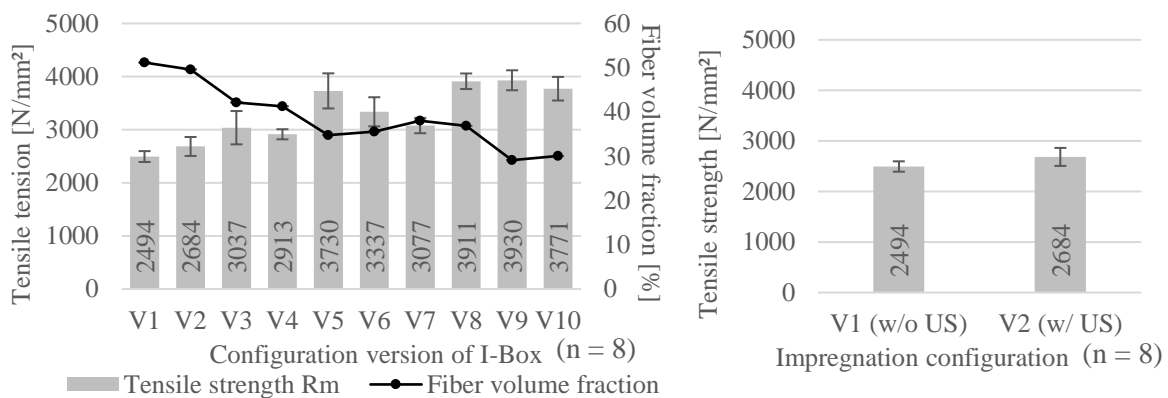
lowest tensile strength of 2,494 N/mm<sup>2</sup> (V1) appears if there is no functional arc length due to the absence of functional elements (e.g., spreading rollers) for shortening the flow paths or enhancement of molecular or particle motion. The applied yarn tensile force has an impact on the tensile strength as well. The diagram in Figure 8b thus show that there is a tendency for tensile strength to decrease with increasing yarn tension. So, the tensile strength difference between the 5.0 N variant (3,730 N/mm<sup>2</sup>) and the 10.0 N variant (3,252 N/mm<sup>2</sup>) is 12%. The difference between the 5.0 N variant and the 7.5 N variant (3,705 N) is inconclusive and accordingly unusable.



(a) Tensile strength versus functional arc length of various impregnation variants (b) Tensile strength depending on different yarn tensile forces for batch V5

Figure 8: Tensile strength with one standard deviation (arc length (a) and yarn tensile force (b))

Another subject of investigation was the influence of ultrasonic vibration on the tensile strength of the impregnated roving (see Figure 9). The basic idea was to enhance the impregnation quality and thus the tensile strength without the use of any other filament-damaging spreading rollers. The results are shown in Figure 9b, whereby the designation “w/o US” means without ultrasonic agitation and “w/ US” means with ultrasonic agitation. The comparison of the two impregnation variants shows only a slight difference, as the V1 (without US) displays a lower tensile strength with 2,494 N/mm<sup>2</sup> compared to V2 (with US) with 2,684 N/mm<sup>2</sup> (+ 7.1%). Environmental factors such as the air pressure, the humidity, and the temperature couldn’t be influenced, so these are potential sources of errors during the testing.



(a) Tensile strength versus FVF (b) Tensile strength depending on ultrasound

Figure 9: Tensile strength with one standard deviation (FVF (a) and external impact of ultrasound (b))

The result of the constructive development process and thus the preferred solution for the I-Box is shown in Figure 10a. The full functional module for yarn guiding and impregnation attached to the industrial robot with its submodules for yarn storage and guiding as well as for the storage, transportation, and regulation of the impregnation agent is depicted in Figure 10b.

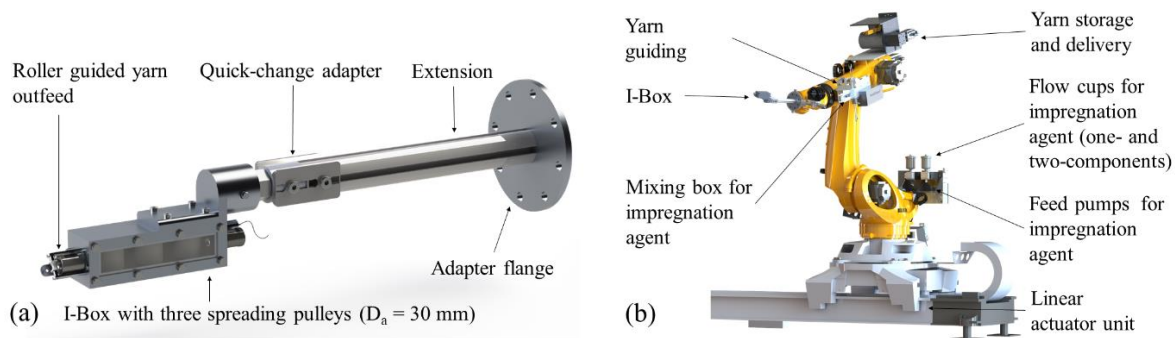


Figure 10: (a) Developed impregnation box; (b) Impregnation box attached to the industrial robot

## CONCLUSIONS

In order to be able to produce complex, highly branched, and biologically inspired 3D textile structures the robot-assisted technology required an innovative roving impregnation module to homogeneously impregnate the carbon fiber roving with maximum freedom of movement for the robot. The experimental investigations led to the important technological finding that the functional elements such as spreading rollers are needed to improve the impregnation probabilities of an I-Box. The initial hypothesis from the preliminary investigations was proven by an extensive investigation design. It can be concluded that the tensile strength of the impregnated carbon fiber roving can be significantly increased with increasing functional arc length as a result of yarn deflection(s). The functional sheet length is determined by the number of deflection bodies, their diameter, their position, and the yarn feed direction. The yarn tension during impregnation also tends to influence the tensile strength. Accordingly, the yarn tensile strength decreases with increasing yarn tension. The results of the experimental investigations were subsequently incorporated into the design development process. The developed I-Box with its modular and minimalistic design enables excellent yarn impregnation quality with very high mechanical properties and great freedom of robot movement without leakage of impregnation agent. The preferred solution provides for three spreader rollers, each with a diameter of 30 mm.

Future subjects of investigations may be a more differentiated analysis of the influence of each functional element, such as differently acting ultrasonic elements (plate transducer compared to rod transducer). Furthermore, the investigation of the same functional elements with different finish roughnesses may be of scientific interest with regard to an improvement of the mechanical characteristics. A hypothesis is given about the functional arc length, but no statement can be made about the effects of certain impregnation configurations with the same functional sheet length but with different numbers of rollers or roller diameters. Furthermore, after the impregnation unit has been installed on the robot and commissioned, functional tests will be carried out which will allow statements to be made on process stability and structure-property relationships.

## ACKNOWLEDGEMENT

Funded by the Deutsche Forschungsgemeinschaft (DFG, German Research Foundation) – SFB/TRR280, Project-ID 417002380. In addition, the authors would like to thank Ziyue Yang for his support as part of his student research project. Copyright of all images: ITM – TU Dresden

## CONFLICT OF INTEREST

The authors declare that they have no conflicts of interest associated with the work presented in this paper.

## DATA AVAILABILITY

The data on which this paper is based are available from the authors on reasonable request.

## References

- Adam, V., Bielak, J., Dommès, C., Will, N., & Hegger, J. (2020). Flexural and Shear Tests on Reinforced Concrete Bridge Deck Slab Segments with a Textile-Reinforced Concrete Strengthening Layer. *MATERIALS*, *13*(18). <https://doi.org/10.3390/ma13184210>
- Beckmann, B., Bielak, J., Scheerer, S., Schmidt, C., Hegger, J., & Curbach, M. (2021). Standortübergreifende Forschung zu Carbonbetonstrukturen im SFB/TRR 280. *Bautechnik*, *98*(3), 232–242. <https://doi.org/10.1002/bate.202000116>
- Beyond Zero Emissions. (2017). *Rethinking cement: Zero carbon industry plan*. Beyond Zero Emissions Inc.
- Cherif, C [Chokri] (Ed.). (2016). *Textile Materials for Lightweight Constructions*. Springer Berlin Heidelberg. 2023-05-15 <https://doi.org/10.1007/978-3-662-46341-3>
- Crippa, M., Oreggioni, G., Guizzardi, D., Muntean, M., Schaaf, E., Lo Vullo, E., Solazzo, E., Monforti-Ferrario, F., Olivier, J., & Vignati, E. (2019). *Fossil CO2 and GHG emissions of all world countries: 2019 report*. EUR: Vol. 29849. Publications Office of the European Union.
- Curbach, M. (2019). *HANDBUCH CARBONBETON: Einsatz nichtmetallischer bewehrung*. WILHELM ERNST & Sohn VERL.
- Deutsches Institut für Normung e.V. (2009 - 08). *DIN 488-1:2009-08: Reinforcing steels - Part 1: Grades, properties, marking (DIN 488-1)*. Berlin. Beuth Verlag GmbH. <https://www.beuth.de/en/standard/din-488-1/117493908>
- DIN Deutsches Institut für Normung e.V. (2004-11). *Carbon fibre: Determination of tensile properties of resin-impregnated yarn (DIN EN ISO 10618)*. Berlin. Beuth Verlag GmbH. <https://www.beuth.de/de/norm/din-en-iso-10618/73061591>
- DIN Deutsches Institut für Normung e.V. (2008-08). *Plastics: Standard atmospheres for conditioning and testing (DIN EN ISO 291)*. Berlin. Beuth Verlag GmbH. <https://www.beuth.de/de/norm/din-en-iso-291/108751092>
- DIN Deutsches Institut für Normung e.V. (2022-11). *Textile-glass-reinforced plastics: Prepregs, moulding compounds and laminates - Determination of the textile-glass and mineral-filler content - Calcination methods (DIN EN ISO 1172)*. Berlin. Beuth Verlag GmbH.
- Dreyer, T. (2022, August 19). Interview by D. Friese [Video call]. Dresden.
- UN Environment Programme. (2021, October 19). *2021 Global Status Report For Buildings and Construction*. <https://globalabc.org/resources/publications/2021-global-status-report-buildings-and-construction>
- Friese, D., Hahn, L., & Cherif, C [Chokri] (2022). Biologically Inspired Load Adapted 3D Textile Reinforcement Structures. *Materials Science Forum*, *1063*, 101–110. <https://doi.org/10.4028/p-80a718>
- Friese, D., Scheurer, M., Hahn, L., Gries, T., & Cherif, C [Chokri] (2022). Textile reinforcement structures for concrete construction applications—a review. *Journal of Composite Materials*, *56*(26), 4041–4064. <https://doi.org/10.1177/00219983221127181>
- Gagg, C. R. (2014). Cement and concrete as an engineering material: An historic appraisal and case study analysis. *ENG FAIL ANAL*, *40*, 114–140. <https://doi.org/10.1016/j.engfailanal.2014.02.004>
- Hahn. (2020). *Entwicklung einer In-situ-Beschichtungs- und Trocknungstechnologie für multiaxiale Gelegestrukturen mit hohem Leistungsvermögen*. Dissertation. TUDpress.
- Hahn, L., Zierold, K., Golla, A., Friese, D., & Rittner, S. (2023). 3D Textiles Based on Warp Knitted Fabrics: A Review. *Materials (Basel, Switzerland)*, *16*(10), 3680. <https://doi.org/10.3390/ma16103680>

- Helbig, T., Unterer, K., Kulas, C., Rempel, S., & Hegger, J. (2016). Fuß- und Radwegbrücke aus Carbonbeton in Albstadt-Ebingen. *BETON- STAHLBETONBAU*, 111(10), 676–685. <https://doi.org/10.1002/best.201600058>
- Knippers, J., Koslowski, V., Solly, J., & Fildhuth, T. (2016). Modular coreless filament winding for lightweight systems in architecture. In CICE (Ed.), *CICE 2016 8th International Conference on Fibre-Reinforced Polymer (FRP) Composites in Civil Engineering*. [https://www.researchgate.net/publication/313421984\\_MODULAR\\_CORELESS\\_FILAMENT\\_WINDING\\_FOR\\_LIGHTWEIGHT\\_SYSTEMS\\_IN\\_ARCHITECTURE](https://www.researchgate.net/publication/313421984_MODULAR_CORELESS_FILAMENT_WINDING_FOR_LIGHTWEIGHT_SYSTEMS_IN_ARCHITECTURE)
- Koutas, L. N., Tetta, Z., Bournas, D. A., & Triantafillou, T. C. (2019). Strengthening of Concrete Structures with Textile Reinforced Mortars: State-of-the-Art Review. *J COMPOS CONSTR*, 23(1), 3118001. [https://doi.org/10.1061/\(ASCE\)CC.1943-5614.0000882](https://doi.org/10.1061/(ASCE)CC.1943-5614.0000882)
- Kulas, C. H. (2013). *Zum Tragverhalten getränkter textiler Bewehrungselemente für Betonbauteile* [Dissertation, Rheinisch-Westfälische Technische Hochschule Aachen, Aachen]. München Technische Universität (TUM).
- May, S., Steinbock, O., Michler, H., & Curbach, M. (2019). Precast Slab Structures Made of Carbon Reinforced Concrete. *Structures*, 18, 20–27. <https://doi.org/10.1016/j.istruc.2018.11.005>
- Mechtcherine, V., Michel, A., Liebscher, M., Schneider, K., & Großmann, C. (2020). Mineral-impregnated carbon fiber composites as novel reinforcement for concrete construction: Material and automation perspectives. *Automation in Construction*, 110, 103002. <https://doi.org/10.1016/j.autcon.2019.103002>
- Meier, R. F. J. (2017). *Über das Fließverhalten von Epoxidharzsystemen und vibrationsunterstützte Harzfiltrationsprozesse* [Dissertation]. Technische Universität München, München. <https://mediatum.ub.tum.de/doc/1329069/document.pdf>
- Minsch, N., Müller, M., Gereke, T., Nocke, A., & Cherif, C [C.] (2018). Novel fully automated 3D coreless filament winding technology. *J COMPOS MATER*, 52(22), 3001–3013. <https://doi.org/10.1177/0021998318759743>
- Raupach, M., & Morales Cruz, C. (2016). Textile-reinforced concrete: Selected case studies. In *Textile Fibre Composites in Civil Engineering* (pp. 275–299). Elsevier. <https://doi.org/10.1016/B978-1-78242-446-8.00013-6>
- Scheerer, S. (2015). Was ist Textilbeton? Eine kurze Einführung in das Thema. *Beton- Und Stahlbetonbau*, 110(S1), 4–7. <https://doi.org/10.1002/best.201400104>
- Schladitz, F., Lorenz, E., Jesse, F., & Curbach, M. (2009). Verstärkung einer denkmalgeschützten Tonnenschale mit Textilbeton. *BETON- STAHLBETONBAU*, 104(7), 432–437. <https://doi.org/10.1002/best.200908241>
- Scholzen, A., Chudoba, R., & Hegger, J. (2015). Thin-walled shell structures made of textile-reinforced concrete. *STRUCT CONCRETE*, 16(1), 106–114. <https://doi.org/10.1002/suco.201300071>
- Sika Deutschland GmbH. (2016). *Biresin CR84 (Compositeharz-System): Technical datasheet*. [www.sika.de](http://www.sika.de)
- Teijin Limited. (2020). *Tenax Filament Yarn: Technical datasheet*. [https://www.tejincarbon.com/fileadmin/PDF/Datenblätter\\_en/Product\\_Data\\_Sheet\\_TSG01en\\_E\\_U\\_Filament\\_.pdf](https://www.tejincarbon.com/fileadmin/PDF/Datenblätter_en/Product_Data_Sheet_TSG01en_E_U_Filament_.pdf)
- Tietze, M., Kirmse, S., Kahnt, A., Schladitz, F., & Curbach, M. (2022). The ecological and economic advantages of carbon reinforced concrete - using the C3 result house CUBE especially the BOX value chain as an example. *Civil Engineering Design*, Article cend.202200001. Advance online publication. <https://doi.org/10.1002/cend.202200001>
- Wulfhorst, B., Gries, T., & Veit, D. (2014). *Textile Fertigungsverfahren: Eine Einführung*. 2., überarbeitete und erweiterte Auflage (2., überarb. u. erw. Aufl.). Carl Hanser Verlag.

Wunnenberg, J., Rjosk, A., Neinhuis, C., & Lautenschläger, T. (2021). Strengthening Structures in the Petiole-Lamina Junction of Peltate Leaves. *Biomimetics (Basel, Switzerland)*, 6(2). <https://doi.org/10.3390/biomimetics6020025>